

High Dispersion Spectroscopy of the Superflare Star KIC6934317 *

Shota NOTSU¹, Satoshi HONDA^{2,3}, Yuta NOTSU¹, Takashi NAGAO¹, Takuya SHIBAYAMA¹,
Hiroyuki MAEHARA^{2,4}, Daisaku NOGAMI², and Kazunari SHIBATA²

¹*Department of Astronomy, Faculty of Science, Kyoto University, Kitashirakawa-Oiwake-cho,
Sakyo-ku, Kyoto 606-8502*

²*Kwasan and Hida Observatories, Kyoto University, Yamashina-ku, Kyoto 607-8471*

³*Center for Astronomy, University of Hyogo, 407-2, Nishigaichi, Sayo-cho, Sayo, Hyogo 679-5313*

⁴*Kiso Observatory, Institute of Astronomy, School of Science, The University of Tokyo, 10762-30,
Mitake, Kiso-machi, Kiso-gun, Nagano 397-0101
snotsu@kwasan.kyoto-u.ac.jp*

(Received 2013 February 8; accepted 2013 July 18)

Abstract

We conducted the high-resolution spectroscopic observation with Subaru/HDS for a G-type star (KIC6934317). We selected this star from the data of the Kepler spacecraft. This star produces a lot of superflares, and the total energy of the largest superflare on this star is $\sim 10^3$ times larger ($\sim 2.2 \times 10^{35}$ erg) than that of the most energetic flare on the Sun ($\sim 10^{32}$ erg). The core depth and emission flux of Ca II infrared triplet lines and H α line show high chromospheric activity in this star, in spite of its low lithium abundance and the small amplitude of the rotational modulation. Using the empirical relations between emission flux of chromospheric lines and X-ray flux, this star is considered to show much higher coronal activity than that of the Sun. It probably has large starspots which can store a large amount of magnetic energy enough to give rise to superflares. We also estimated the stellar parameters, such as effective temperature, surface gravity, metallicity, projected rotational velocity ($v \sin i$), and radial velocity. KIC6934317 is then confirmed to be an early G-type main sequence star. The value of $v \sin i$ is estimated to be ~ 1.91 km s⁻¹. In contrast, the rotational velocity is calculated to be ~ 20 km s⁻¹ by using the period of the brightness variation as the rotation period. This difference can be explained by its small inclination angle (nearly pole-on). The small inclination angle is also supported by the contrast between the large superflare amplitude and the small stellar brightness variation amplitude. The lithium abundance and isochrones implies that the age of this star is more than about a few Gyr, though a problem why this star with such an age has a strong activity remains unsolved.

Key words: stars: flare — stars: chromospheres — stars: activity — stars: spots
— stars: rotation

1. Introduction

Flares are explosions on the stellar surface, and are thought to occur by intense release of magnetic energy stored near starspots (e.g., Shibata & Magara 2011). The typical amount of energy released in solar flares is $10^{29} - 3 \times 10^{32}$ erg (e.g., Priest 1981; Shibata & Yokoyama 2002).

Schaefer, King, Deliyannis (2000) found 9 candidates of superflares on slowly rotating stars like the Sun. Superflares are the flares whose total energy is $10 - 10^6$ times larger ($\sim 10^{33} - 10^{38}$ erg) than that of the most energetic flare on the Sun ($\sim 10^{32}$ erg). Recently, Maehara et al. (2012) discovered 365 superflare events on 148 solar-type stars that have effective temperature of $5100\text{K} \leq T_{\text{eff}} < 6000\text{K}$, and surface gravity of $\log g \geq 4.0$ by analyzing the data of the Kepler spacecraft (Koch et al. 2010). In addition, Shibayama et al. (2013) discovered 1547 superflares on 279 solar-type stars. The Kepler spacecraft is particularly suitable for the detection of flares of small intensity, against the integrated star disk brightness, because of the combination of high photometric accuracy (10^{-6} mag) and continuous time-series data of a lot of stars over a long period (e.g., Walkowicz et al. 2011; Balona 2012).

Maehara et al. (2012) and Shibayama et al. (2013) suggested that superflares releasing a total energy in the range $\sim 10^{34} - 10^{35}$ erg can occur once in 800 – 5000 years on Sun-like stars that have effective temperature of $5600\text{K} \leq T_{\text{eff}} < 6000\text{K}$, surface gravity of $\log g \geq 4.0$, and the rotational period of $P \geq 10$ days. Many of solar-type stars having superflares show quasi-periodic brightness variations with a typical period from one day to a few tens of days. The amplitude of the brightness variations is in the range 0.1~10% (Maehara et al. 2012; Shibayama et al. 2013). Such brightness variations can be explained by the rotation of the star having starspots (e.g., Basri et al. 2011; Debosscher et al. 2011; Harrison et al. 2012).

Notsu et al. (2013) found that the brightness variations of superflare-generating stars can be well explained by the rotation of the star with fairly large starspots, taking into account the effects of inclination angle and spot latitude. They also confirmed the correlation between the starspot coverage and the maximum energy of superflares. These results indicate that the energy of superflares can be explained by the magnetic energy stored around the starspots. In addition, Shibata et al. (2013) suggested from theoretical estimates that the Sun can generate

* Based on data collected at Subaru Telescope, which is operated by the National Astronomical Observatory of Japan.

large magnetic flux which is enough for causing superflares with energy of 10^{34} erg within one solar cycle period (~ 11 years).

If such large starspots exist on a star, the activity level of its chromosphere becomes high and large plages occur near the starspots (Shine & Linsky 1972). Linsky et al. (1979) and Foing et al. (1989) suggested that the lines of Ca II infrared triplet (Ca II IRT, $\lambda = 8498, 8542, 8662\text{\AA}$) indicate the chromospheric activity of G-type stars. This is because these are collision-dominated lines and their cores are formed in the chromosphere, reflecting the temperature rise in their profiles which go from filled-in to pure emission, depending on the activity level. The fluxes in these lines are known to correlate well with the Ca II H+K emission index ($\log R'_{\text{HK}}$) and emission flux, which has been used as the indicator of chromospheric activity more traditionally (e.g., Rutten 1984; Schrijver et al. 1992; Chmielewski 2000; Busà et al. 2007; Hall 2008; Martínez-Arnáiz et al. 2011; Takeda et al. 2012). Solar imaging spectroscopy in these lines is also conducted to investigate chromospheric structures, such as plages and fibrils (e.g., Shine & Linsky 1972; Cauzzi et al. 2008; Reardon et al. 2009).

In addition, Herbig (1985), Soderblom et al. (1993b), and Frasca et al. (2010) suggested that the $H\alpha$ line also indicates the chromospheric activity of the Sun and G-type stars. This is because the optical depth in the line core is large, and because the line formation becomes more and more dominated by collisions in very active stars or in plage regions. Therefore, it is very important to conduct high-resolution spectroscopic observations to investigate the chromospheric activity of stars generating superflares, which is related to their photospheric starspots.

In this research, we analyze the high-resolution spectrum of a G-type superflare star (KIC6934317), and investigate the chromospheric activity and the presence of starspots. We also estimate stellar parameters of the star, such as T_{eff} , $\log g$, metallicity represented by the Fe abundance relative to the Sun ($[\text{Fe}/\text{H}]$)¹, projected rotational velocity ($v \sin i$) and the radial velocity (RV), and discuss some features of this star. This is the first high-resolution spectroscopic study of G-type superflare-generating stars discovered by Kepler spacecraft.

We discuss the selection of the target and our high-resolutions spectroscopic observation in Section 2. We show the method to measure stellar parameters in Section 3. The results of

¹ $[\text{Fe}/\text{H}]$ is presented by the following relation,

$$[\text{Fe}/\text{H}] = \log(N_{\text{Fe}}/N_{\text{H}})_{\text{star}} - \log(N_{\text{Fe}}/N_{\text{H}})_{\text{sun}}, \quad (1)$$

where $(N_{\text{Fe}}/N_{\text{H}})_{\text{star}}$ is the ratio of the number of Iron (Fe) atoms to that of Hydrogen (H) atoms in the star, and $(N_{\text{Fe}}/N_{\text{H}})_{\text{sun}}$ is the same ratio in the Sun. Asplund et al. (2009) reported that $\log(N_{\text{Fe}}/N_{\text{H}})_{\text{sun}}$ is -4.5 ± 0.04 .

stellar parameters, such as chromospheric parameters and $v \sin i$, are reported in Section 4. Finally in Section 5, we discuss the stellar activity, the rotational velocity, and the binarity of this star.

2. Targets and Observation

2.1. Target Selection

We selected the G-type superflare star (KIC6934317) as the target. This star exhibited 48 superflares in about 617 days, and hence the superflare occurrence frequency of this star is about once in 13 days. We selected the star from the data of the Kepler spacecraft (Koch et al. 2010) within the temperature range between 5100K to 6000K. These Kepler data were retrieved from the Multimission Archive at Space Telescope Science Institute (MAST)². In addition, we applied the analysis methods described in Maehara et al. (2012) and Shibayama et al. (2013) to search for superflares. According to KIC (Kepler Input Catalog, Brown et al. 2011), this star is 12.03 mag in the i band and was the brightest superflare star at present in our data. Table 1 shows the photometric data of KIC6934317 taken from previous studies in detail. The UBV magnitudes are taken from the photometric survey of the Kepler Field³ (Everett et al. 2012), and those of JHK_s magnitudes are from the data of Two Micron All Sky Survey (2MASS; Skrutskie et al. 2006). The atmospheric parameters reported in the KIC (Brown et al. 2011) are $T_{\text{eff}} = 5387 \pm 200\text{K}$, $\log g = 3.8 \pm 0.4$. They also quote a radius of $2.3R_{\odot}$.

Figure 1(a) shows the light curve of KIC6934317 and reveals a quasi-periodic brightness variation. The amplitude of this variation is small ($\sim 0.1\%$) compared to those of other stars which undergo superflares. Figure 1(b) is an enlarged lightcurve of a superflare observed around BJD 2455257.9. The amplitude of this flare is about 2.1% of the brightness of this star, the duration of the flare is about 0.12 day, and the total radiative energy during this event is about 5.6×10^{34} erg. Maehara et al. (2012) and Shibayama et al. (2013) described the method of estimating the total energy of each flare in detail. The largest superflare on KIC6934317 was observed around BJD 2455735.3. Its amplitude is about 5.7% of the brightness of this star, the duration of this flare is about 0.10 day, and the total radiative energy released during this event is about 2.2×10^{35} erg. Figure 1(c) shows the power spectrum of the time variation of the stellar brightness of KIC6934317 and it shows that the period of the brightness variation (P_s) is about 2.54 days.

² <http://archive.stsci.edu/kepler/>

³ The data of this survey is available at http://archive.stsci.edu/kepler/kepler_fov/search.php/.

We also selected 59Vir and 61Vir as references of G-type stars. Previous studies (e.g., Anderson et al. 2010) have shown that 59Vir rotates rather fast and has strong magnetic fields ($\sim 500\text{G}$), while 61Vir is slowly rotating and no magnetic field could be detected.

Table 2 shows in detail some stellar parameters (atmospheric parameters, projected rotational velocity, radial velocity, and lithium abundance) of KIC6934317 taken from previous studies and derived in this study, and Table 3 shows those of our comparison stars (59Vir, 61Vir).

2.2. Subaru Observations and Data Reduction

We carried out high dispersion spectroscopy of KIC6934317, 59Vir, and 61Vir on August 3, 2011 (Hawaii Standard Time) in Subaru service program in semester 11B (S11B-137S). We used High Dispersion Spectrograph (HDS: Noguchi et al. (2002)) at the 8.2-m Subaru telescope. The spectral coverage was about $6100\text{\AA}\sim 8820\text{\AA}$. This range includes important lines, such as those of Ca II infrared triplet ($8498, 8542, 8662\text{\AA}$), $\text{H}\alpha$ (6562.8\AA), the Li I line (6708\AA), and some lines of Fe I and Fe II (for measuring atmospheric parameters, projected rotational velocity, and radial velocity). The exposure time of KIC6934317 was 1800×6 seconds to get signal-to-noise (S/N) ratio as ~ 150 at 8520\AA (around the Ca II IRT lines), and as ~ 210 at 6700\AA (around the line of Li I 6708\AA). The exposure times of 59Vir and 61Vir were 60×2 seconds per each star. S/N ratio of 59Vir is ~ 370 at 8520\AA and ~ 540 at 6700\AA and that of 61Vir is ~ 410 at 8520\AA and ~ 690 at 6700\AA .

The spectral resolution, as evaluated from the full width at half maximum (FWHM) of the emission lines of the Th-Ar calibration lamp, was 0.088\AA at 8500\AA , yielding a resolving power $R=\lambda/\Delta\lambda\sim 97,000$ (for the slit width of 0.36 arcsec).

The data reduction (bias subtraction, flat fielding, aperture determination, scattered light subtraction, spectral extraction, wavelength calibration, and normalization by the continuum) was performed with the ECHELLE package of the IRAF⁴ software.

Figure 2 shows the lightcurve of KIC6934317 around the period of this observation (around BJD 2455778). The spectrum was taken during the minimum of the wave-like modulation. There was a large flare about a day before the observation period.

⁴ IRAF is distributed by the National Optical Astronomy Observatories, which is operated by the Association of Universities for Research in Astronomy, Inc., under cooperate agreement with the National Science Foundation.

3. Measurements of Stellar Parameters

3.1. Atmospheric Parameters

We measured equivalent widths of 101 Fe I lines and 7 Fe II lines over the range of 6100–7400Å of the target stars (KIC6934317, 59Vir, and 61Vir). These Fe I and II lines are selected from the line list presented in Takeda et al. (2005b), which is based on many previous studies (e.g., Kurucz et al. 1984; Meylan et al. 1993; Kurucz & Bell 1995). In this process of measuring equivalent widths, we used the code SPSHOW contained in SPTOOL software package⁵ developed by Y. Takeda. Programs contained in SPTOOL are originally based on Kurucz’s ATLAS9/WIDTH9 model atmospheric programs (Kurucz 1993).

Using these data of equivalent widths of Fe I and Fe II lines, we derived the effective temperature (T_{eff}), the surface gravity ($\log g$), microturbulent velocity (v_t), and $[\text{Fe}/\text{H}]$ of target stars. For deriving these parameters, we used TGVIT program⁶ developed by Y. Takeda. The procedures adopted in this program are minutely described in Takeda, Ohkubo, Sadakane (2002) and Takeda et al. (2005b).

The resultant parameters of T_{eff} , $\log g$, v_t , and $[\text{Fe}/\text{H}]$ of KIC6934317 are $5694 \pm 25\text{K}$, 4.42 ± 0.08 , $0.87 \pm 0.14 \text{ km s}^{-1}$, and -0.03 ± 0.07 , respectively. On the other hand, the atmospheric parameters reported in the KIC (Brown et al. 2011) are $T_{\text{eff}} = 5387 \pm 200\text{K}$, $\log g = 3.8 \pm 0.4$, and $[\text{Fe}/\text{H}] = -0.78 \pm 0.5$. There are significant differences between the values reported in the KIC and those derived in this observation. However, the atmospheric parameters reported in the KIC are derived from multiband photometry for a first classification and are not good sources to discuss actual properties of the stars. Furthermore, it is known that in some cases the atmospheric parameters taken from the KIC are significantly different from those derived spectroscopically, which are much more accurate than those from the KIC (e.g., Molenda-Żakowicz et al. 2010, Pinsonneault et al. 2012).

In addition, the resultant parameters of 59Vir are $T_{\text{eff}} = 6009 \pm 28\text{K}$, $\log g = 4.15 \pm 0.06$, $v_t = 1.32 \pm 0.09 \text{ km s}^{-1}$, and $[\text{Fe}/\text{H}] = 0.09 \pm 0.06$, and those of 61Vir are $T_{\text{eff}} = 5558 \pm 15\text{K}$, $\log g = 4.50 \pm 0.04$, $v_t = 0.87 \pm 0.08 \text{ km s}^{-1}$, and $[\text{Fe}/\text{H}] = -0.04 \pm 0.06$. These values are consistent with those of previous studies (e.g., Takeda 2007a; Schröder et al. 2009; Anderson et al. 2010). Obviously, the errors of the parameters are internal to the procedure and do not

⁵ <http://optik2.mtk.nao.ac.jp/~takeda/sptool/>

⁶ <http://optik2.mtk.nao.ac.jp/~takeda/tgv/>

include any systematic effect due to the choice of the line-list and the model atmosphere.

For the sake of checking the accuracy of the atmospheric parameters derived from equivalent widths of Fe I and Fe II lines, we also estimated T_{eff} from the ratio of the depth of two different lines (e.g., Biazzo et al. 2007). We measured the line-depth ratio of three pairs of lines (V I 6199Å/Fe I 6200Å, V I 6214Å/Fe I 6213Å, and V I 6275Å/Fe I 6270Å), and roughly estimated the average values of T_{eff} by using the method described in Biazzo et al. (2007). The value of T_{eff} of KIC6934317, 59Vir and 61Vir is $\sim 5850\text{K}$, $\sim 6060\text{K}$, and $\sim 5800\text{K}$, respectively. These values are roughly consistent with the values of T_{eff} derived from equivalent widths of Fe I and Fe II lines.

Pinsonneault et al. (2012) reported a catalog⁷ of revised T_{eff} for stars in the KIC (Brown et al. 2011). They estimated T_{eff} by using two different methods and compared their values with those in the KIC. In one method, they transformed original *griz* colors in the KIC into *griz* colors on the basis of Sloan Digital Sky Survey (SDSS; Aihara et al. 2011) scales and calculated T_{eff} from the relations between SDSS *griz* colors and T_{eff} . Hereafter, we refer to this method as the SDSS one. In the other method, T_{eff} is derived with the infrared flux method (IRFM; e.g., Casagrande et al. 2010) which uses the relations between T_{eff} and $J - K$ s from the data of 2MASS (Skrutskie et al. 2006). We call this the IRFM method. The effects of interstellar reddening are also corrected in these two methods of estimating T_{eff} (Casagrande et al. 2010, Pinsonneault et al. 2012). They argued that these revised values of T_{eff} with two different methods are both about 200K higher than the values of T_{eff} in the KIC, and these revised values are comparable with the values derived spectroscopically.

According to this catalog, the revised T_{eff} of KIC6934317 by using the SDSS method is $5710 \pm 81\text{K}$, and the value with the IRFM method is $5604 \pm 103\text{K}$. These revised values are higher than that in the KIC, and are consistent with the result of this spectroscopic observation within the error range.

On the basis of results derived spectroscopically, KIC6934317 is an early G-type main sequence star, and T_{eff} , $\log g$, and $[\text{Fe}/\text{H}]$ of this star are nearly the same as the Sun. Atmospheric parameters of KIC6934317 taken from previous studies and derived in this study are shown in Table 2, and those of comparison stars (59Vir, 61Vir) are shown in Table 3.

⁷ This catalog is available at <http://vizier.cfa.harvard.edu/viz-bin/VizieR-3>.

3.2. $v \sin i$

We used the method which is basically similar to that described in Takeda, Sato, Murata (2008) in order to derive $v \sin i$ of KIC6934317, the Sun, 59Vir, and 61Vir. In this process of calculating $v \sin i$, we took into account the macroturbulence velocity and instrumental broadening velocity on the basis of Takeda, Sato, Murata (2008). We used the spectrum of the Sun in Kurucz et al. (1984) to calculate $v \sin i$ of the Sun.

According to Takeda, Sato, Murata (2008), a simple relation holds among the line-broadening parameters, which can be expressed as:

$$v_M^2 = v_{ip}^2 + v_{rt}^2 + v_{mt}^2. \quad (2)$$

v_M is e -folding width of the Gaussian macrobroadening function [$f(v) \propto \exp(-(v/v_M)^2)$] including instrumental broadening (v_{ip}), rotation (v_{rt}), and macroturbulence (v_{mt}). We derived v_M by applying automatic spectrum-fitting technique, given the model atmosphere corresponding to the atmospheric parameters (e.g, Takeda 1995; Takeda 2007a; Takeda et al. 2008). In this process, we used the MPFIT program contained in SPTOOL software package. Although Takeda, Sato, Murata (2008) applied this fitting technique to the 6080-6089Å region, we applied this technique to the 6212-6220Å region, which contains four Fe I lines. This is because the 6080-6089Å region is out of the spectral coverage of our observation. In deriving v_M of KIC6934317, 59Vir, and 61Vir, we used the atmospheric parameters derived in Section 3.1 (See also Table 2 and 3). In order to calculate v_M of the Sun, we used the values of atmospheric parameters in Kurucz (1993) ($\log g = 4.44$, $T_{\text{eff}} = 5777\text{K}$). We also determined v_t of the Sun is 1 km s^{-1} .

v_{ip} is e -folding width of the Gaussian instrumental broadening function. v_{ip} was calculated by using the following relation (Takeda, Sato, Murata 2008),

$$v_{ip} = \frac{3 \times 10^5}{2R\sqrt{\ln 2}}, \quad (3)$$

where R is a resolving power of the observation. v_{mt} is e -folding width of the Gaussian macroturbulence broadening function. v_{mt} was estimated by using the relation, $v_{mt} \sim 0.42\zeta_{\text{RT}}$ (Takeda, Sato, Murata (2008)). ζ_{RT} is the radial tangential macroturbulence and we calculated ζ_{RT} by the relation (Valenti & Fischer 2005),

$$\zeta_{\text{RT}} = \left(3.98 - \frac{T_{\text{eff}} - 5770\text{K}}{650\text{K}} \right), \quad (4)$$

where T_{eff} is the effective temperature of stars.

Using these equations, we derived v_{rt} , which is e -folding width of the Gaussian rotational broadening function, and finally we could derive $v \sin i$ by using the relation $v_{rt} \sim 0.94v \sin i$

between v_{rt} and $v \sin i$ (Gray 2005). Hirano et al. (2012) estimated the systematic uncertainty for $v \sin i$ by changing ζ_{RT} by $\pm 15\%$ from Equation (4) for cool stars ($T_{\text{eff}} \leq 6100\text{K}$) on the basis of observed distribution of ζ_{RT} (See also Figure 3 in Valenti & Fischer 2005). They explained that the statistical errors in fitting each spectrum are generally smaller than the systematic errors arising from different values of ζ_{RT} .

3.3. Measurements of Ca II Infrared Triplet (Ca II IRT) and H α

In order to investigate the chromospheric activity of the target stars, we used $r_0(8498)$, $r_0(8542)$, and $r_0(8662)$, which are the residual flux normalized by the continuum at the line cores of Ca II Infrared Triplet (Ca II IRT, $\lambda = 8498, 8542, 8662\text{\AA}$). As the chromospheric activity is enhanced and plages appear, $r_0(8498)$, $r_0(8542)$, and $r_0(8662)$ become large, since a greater amount of emission from the chromosphere fills in the core of the lines (e.g., Linsky et al. 1979; Foing et al. 1989; Takeda et al. 2010). These indicators are known to correlate well with the Ca II H+K emission index ($\log R'_{\text{HK}}$), which has been used as the indicator of chromospheric activity more traditionally (e.g., Rutten 1984; Schrijver et al. 1992; Chmielewski 2000; Busà et al. 2007; Hall 2008; Takeda et al. 2012). We also used $r_0(\text{H}\alpha)$ as an indicator of chromospheric activity. Herbig (1985), Soderblom et al. (1993b), and Frasca et al. (2010) described that H α is also a useful indicator of chromospheric activity, and $r_0(\text{H}\alpha)$ is correlated well with Ca II H+K emission index ($\log R'_{\text{HK}}$). On the other hand, Ca II IRT lines are more easily used as diagnostics of chromospheric activity compared to Ca II H&K lines, because they lie in a wavelength region where the continuum is well defined and the spectrograph detectors are more efficient (Frasca et al. 2010).

We also used emission flux of Ca II IRT and H α lines. The residual flux at the cores of Ca II IRT and H α lines, as defined in the previous paragraph, is an indicator of chromospheric activity which is widely used (e.g., Linsky et al. 1979; Foing et al. 1989), but it also depends on the value of $v \sin i$ of the star (e.g., Takeda et al. 2010). A large value of $v \sin i$ can indeed rise the residual flux, mimicking the effect of filling the line core with chromospheric emission. In order to remove this influence of $v \sin i$, we used the spectral subtraction technique (e.g., Frasca & Catalano 1994; Frasca et al. 2011; Martínez-Arnáiz et al. 2011; Fröhlich et al. 2012). Martínez-Arnáiz et al. (2011) pointed out that this subtraction process also permits the subtraction of the underlying photospheric contribution from the spectrum of the star, and in this way we could investigate the spectral emission originated from the chromosphere in detail. We used the spectrum of 61Vir obtained in this observation as an inactive template to be subtracted from the spectrum of KIC6934317. 61Vir is a slowly rotating and non-active early G-type main sequence star (e.g., Anderson et al. 2010), whose atmospheric parameters

are very similar to those of KIC6934317 (See Tables 2 and 3).

We measured the excess equivalent width (W_{λ}^{em}) of the Ca II IRT and H α lines in the residual spectrum resulting from this subtraction process. We subsequently derived emission fluxes (F_{λ}^{em}) of Ca II IRT and H α lines from W_{λ}^{em} of these lines by the following relation, $F_{\lambda}^{\text{em}} = W_{\lambda}^{\text{em}} F_{\lambda}^{\text{cont}}$ (Martínez-Arnáiz et al. (2011)). $F_{\lambda}^{\text{cont}}$ is the continuum flux around the wavelength of each line. We calculated $F_{\lambda}^{\text{cont}}$ by using the the following empirical relationships between $F_{\lambda}^{\text{cont}}$ and color index ($B - V$) derived by Hall (1996),

$$\log F_{\text{H}\alpha}^{\text{cont}} = [7.538 - 1.081(B - V)] \pm 0.033, \quad +0.0 \leq B - V \leq +1.4, \quad (5)$$

$$\log F_{\text{IRT}}^{\text{cont}} = [7.223 - 1.330(B - V)] \pm 0.043, \quad -0.1 \leq B - V \leq +0.22, \quad (6)$$

$$\log F_{\text{IRT}}^{\text{cont}} = [7.083 - 0.685(B - V)] \pm 0.055, \quad +0.22 \leq B - V \leq +1.4. \quad (7)$$

Martínez-Arnáiz et al. (2011) also used the same method to calculate $F_{\lambda}^{\text{cont}}$.

In Section 3.1, we show that KIC6934317 is $T_{\text{eff}} = 5694 \pm 25\text{K}$ and $[\text{Fe}/\text{H}] = -0.03 \pm 0.07$. Alonso et al. (1996) showed the empirical relations of low mass main sequence stars (F0V–K5V) among $[\text{Fe}/\text{H}]$, T_{eff} , and color index. We estimated the unreddened color $(B - V)_0$ of this star as ~ 0.64 by using this relation. Photometric data of this star (Everett et al. 2012) show that KIC6934317 is 13.191 ± 0.023 mag in the B-band and 12.516 ± 0.017 mag in the V-band (See Table 1), and thus $B - V$ simply derived from these photometric data is 0.675 ± 0.040 . The KIC (Brown et al. 2011) reports a value of color excess $E(B - V) = 0.093 \pm 0.1$ mag, which has been estimated with a simple model for the dust distribution in the Milky Way.

The value of $B - V$ estimated from atmospheric parameters derived spectroscopically ($(B - V)_0$) agrees with the corrected value of $B - V$ on the basis of the photometric data within the error range, and is considered to be more accurate than the corrected value on the basis of photometric data. We consequently use the value estimated from atmospheric parameters derived spectroscopically ($(B - V)_0$) and the resulting color excess $E(B - V) \sim 0.04 \pm 0.04$ mag in the following discussions.

Martínez-Arnáiz et al. (2011) described that emission fluxes (F_{λ}^{em}) of Ca II IRT and H α lines are correlated well with one another, and are also correlated well with F_{λ}^{em} of Ca II H & K lines, which have been used as the indicator of chromospheric activity more traditionally (e.g., Rutten 1984; Schrijver et al. 1992; Chmielewski 2000; Busà et al. 2007; Hall 2008; Takeda et al. 2012). Furthermore, F_{λ}^{em} of Ca II IRT, Ca II H & K, and H α lines are correlated well with X-ray surface flux (F_X), which indicates coronal activity (e.g., Schrijver et al. 1992; Martínez-Arnáiz et al. 2011).

4. Results

4.1. Projected Rotational Velocity

Figure 3 shows that the photospheric lines of 59Vir are shallow and broad, indicating 59Vir is a fast rotator. On the other hand, the line of KIC6934317 is narrow and deep like those of 61Vir and the Sun, which rotate slowly. Using the methods explained in Section 3.2, the values of $v \sin i$ of KIC6934317, 59Vir, 61Vir and the Sun are about 1.91, 6.27, 1.38, and 1.82 km s⁻¹, respectively. We show these results in Table 2 and 3. The results of 59Vir and 61Vir of this observation are roughly consistent with those of previous researches which are described in Table 3 (e.g., Anderson et al. 2010, Schröder et al. 2009). In Section 5.2, we discuss the results of $v \sin i$ in detail.

4.2. Radial Velocity

We measured the radial velocity (RV) of the target stars by using about 65 Fe I lines. As we showed in Table 2 and 3, the RV values of KIC6934317, 59Vir, and 61Vir measured on our spectra are -12.238 ± 0.018 , -26.727 ± 0.026 , and -7.528 ± 0.027 km s⁻¹, respectively. These values are derived from the spectra obtained by integrating all frames of spectra of individual stars. The errors of RV values are the standard errors of the mean RV values which are calculated by using the values derived from individual lines. The results for 59Vir and 61Vir agree with those of previous studies (e.g., Takeda et al. 2005a), which are described in Table 3. In Section 5.3, we discuss the results of RV in detail.

4.3. Stellar Age, Mass, Luminosity, Radius, and Distance

In Section 3.1, we derived T_{eff} , $\log g$, and $[\text{Fe}/\text{H}]$ of target stars from our observed spectra. On the basis of these parameters, we can estimate the stellar age, the stellar mass (M_s), the absolute V magnitude (M_V), and the stellar bolometric luminosity (L_s) for the target stars by applying the isochrones of Girardi et al. (2000). In addition, using the values of L_s and T_{eff} , we can also estimate the stellar radius (R_s).

The values of the stellar age, M_s , M_V , L_s , and R_s of KIC6934317 are $\sim 4.5 - 7.0$ Gyr, $\sim 0.97M_\odot$, $\sim 4.9 - 5.0$ mag, $\sim 0.9L_\odot$, and $\sim 1.0R_\odot$, respectively. Though the range of stellar age is wide, this value is roughly similar to the age of the Sun.

In addition, Table 1 shows that the apparent V magnitude of this star is 12.516 ± 0.017 mag. Using the value of $E(B - V)$ estimated in Section 3.3, the value of interstellar extinction in the V band ($A(V)$) is $A(V) = 3.1 \times E(B - V) \sim 0.12 \pm 0.12$ mag (Cardelli et al. 1989). Using these values and M_V , we estimate that the distance of this star (d) is ~ 300 pc.

4.4. Spectra of Ca II Infrared Triplet and $H\alpha$

In the top of Figure 4(a) and 4(b), normalized spectra of KIC6934317, 59Vir and 61Vir around the cores of $\lambda 8498$ and $\lambda 8542 \text{ \AA}$ are represented, respectively. In the bottom of these figures, the spectrum obtained after the subtraction of the inactive template (61 Vir) is represented. The excess emissions in the cores of Ca II 8498 \AA and 8542 \AA are evident in these subtracted spectra.

Using these spectra, we found that $r_0(8498)$ and $r_0(8542)$ of KIC6934317 are larger than those of 61Vir, which rotates slowly and has very weak magnetic field, while they are comparable to those of 59Vir, which rotates fast ($\sim 6.28 \text{ km s}^{-1}$) and has strong magnetic fields. We show $r_0(8498)$, $r_0(8542)$, $r_0(8662)$, and $r_0(H\alpha)$ of KIC6934317, 59Vir, 61Vir, and the Sun in Table 4. The spectrum of the Sun is obtained by Kurucz et al. (1984). The original resolving power ($R = \lambda / \Delta\lambda$) of this solar spectrum is $\sim 500,000$, and we used the corrected solar spectrum which we rebinned from $R \sim 500,000$ to $R \sim 100,000$ to match the resolution of our HDS spectra. This table shows that the difference of $r_0(8498)$ between KIC6934317 and the Sun is 0.14 and the difference of $r_0(8542)$ between KIC6934317 and the Sun is 0.15. This table shows that the tendencies of $r_0(8662)$ and $r_0(H\alpha)$ are similar to those of $r_0(8498)$ and $r_0(8542)$. Chmielewski (2000) reported a value of $r_0(8542) = 0.24$ for 61Vir. Comparing this data with the results described in Table 4, we find that the error range of $r_0(8542)$ is ~ 0.05 . Previous studies (e.g., Linsky et al. 1979; Herbig 1985; Chmielewski 2000) have shown that the values of $r_0(8498)$, $r_0(8542)$, $r_0(8662)$, and $r_0(H\alpha)$ become large as the star shows high chromospheric activity and large plages appear on the star. Altogether, these results suggest that KIC6934317 shows high chromospheric activity like 59Vir.

Table 5 shows the excess equivalent width (W_λ^{em}) of the Ca II IRT and $H\alpha$ lines, and emission flux (F_λ^{em}) of these lines. The values of F_λ^{em} are derived by using the method explained in Section 3.3. In Table 5, we report these values not only of KIC6934317, but also of the stars investigated in Fröhlich et al. (2012) (KIC7985370 and KIC7765135), with the aim of comparing chromospheric activity. Fröhlich et al. (2012) reported that KIC7985370 and KIC7765135 are early G-type main sequence stars. They also reported that these stars are young (Age; 100 – 200 Myr) and show high chromospheric activity. On the basis of the values

in Table 5, $F_{\text{H}\alpha}^{\text{em}}$ of KIC6934317 is roughly as large as of those of KIC7985370 and KIC7765135. In contrast, F_{λ}^{em} of Ca II IRT lines of KIC6934317 are about a few times smaller than those of KIC7985370 and KIC7765135. Consequently, the chromospheric activity of KIC6934317 is fairly high, and this star displays an excess of H α flux with respect to Ca II IRT flux, compared to KIC7985370 and KIC7765135.

In Section 5.1, we further discuss the stellar activity of KIC6934317.

4.5. Spectra of Li I

Figure 5 shows normalized spectra of KIC6934317, 59Vir, 61Vir, and the Sun around the Li I line (6708Å). This figure shows that 59Vir has a deep line of Li, and that the Li line of 61Vir is absent while that of the Sun and KIC6934317 are very weak and just visible against the noise.

We measured the lithium abundance ($A(\text{Li})^8$) of KIC6934317, 59Vir, 61Vir, and the Sun on the basis of the automatic profile fitting method described in details in Takeda & Kawanomoto (2005). In this process of calculating $A(\text{Li})$, we used the MPFIT program contained in SPTOOL software package, and assumed LTE (Local Thermodynamical Equilibrium) for the formation of all lines including the Li I line. We also assumed ${}^6\text{Li}/{}^7\text{Li} = 0$ throughout this study. The line lists we used are the same of Takeda & Kawanomoto (2005).

The result of KIC6934317 is $A(\text{Li})=1.25$. In addition, the result of 59Vir is $A(\text{Li})=2.81$ and that of the Sun is $A(\text{Li})=0.88$. We could not derive $A(\text{Li})$ of 61Vir, because the Li line of 61Vir is absent.

Takeda & Kawanomoto (2005) shows that in the case of calculating $A(\text{Li})$ by LTE, the results of 59Vir are $W_{\text{Li}}^9 = 83.1 \text{ m}\text{\AA}$ and $A(\text{Li})=2.91$, those of the Sun are $W_{\text{Li}} = 2.1 \text{ m}\text{\AA}$ and $A(\text{Li})=0.85$, and those of 61Vir are $W_{\text{Li}} < 2 \text{ m}\text{\AA}$ and $A(\text{Li}) < 0.86$. In the case of calculating $A(\text{Li})$ by NLTE (Non Local Thermodynamical Equilibrium), $A(\text{Li})$ of 59Vir and the Sun are 2.91 and 0.92, respectively. Asplund et al. (2009) also shows that $A(\text{Li})$ of the solar photosphere calculated by NLTE is 1.05 ± 0.10 . In table 2 and 3, we show the values of previous studies and this study. The values of 59Vir, 61Vir, and the Sun of this observation are roughly consistent with those of previous studies. These results show that the lithium abundance

⁸ $A(\text{Li})$ is defined by the following relation,

$$A(\text{Li}) = \log(N_{\text{Li}}/N_{\text{H}}) + 12.00, \quad (8)$$

where $(N_{\text{Li}}/N_{\text{H}})_{\text{star}}$ is the ratio of the number of Lithium (Li) atoms to that of Hydrogen (H) atoms in the star.

⁹ W_{Li} is the equivalent width of the line of Li I 6708Å.

of KIC6934317 is quite lower than that of 59Vir, and a bit higher than that of 61Vir and the Sun.

It has been known that the lithium abundances could provide a fairly rough constraint on the age of early G-type stars (e.g., Soderblom et al. 1993a; Sestito & Randich 2005), though there are a lot of unknown problems about the behavior of lithium abundances in early G-type stars (e.g., Ryan et al. 2001; Israelian et al. 2004; Sestito & Randich 2005; Takeda et al. (2007b); Takeda et al. 2010; Takeda et al. 2012). On the basis of the fairly rough relation between $A(\text{Li})$ and the stellar age discussed in Sestito & Randich (2005), Takeda et al. (2007b), and Takeda et al. (2010), the age of KIC6934317 is more than about a few Gyr. This value is roughly consistent with the age derived by using the isochrones of Girardi et al. (2000) (see Section 4.3), though the ranges of these two values are wide.

5. Discussion

5.1. *Stellar Activity and Superflares*

In Figure 6, we plot $r_0(8542)$ as a function of effective temperature (T_{eff}) of the stars. In making this figure, we use both the results described in Table 4 and the data from Chmielewski (2000). There appears to be a clear dividing gap between active and quiescent stars which show some slope with effective temperature (Foing et al. 1989, Chmielewski 2000). $r_0(8542)$ become large as the activity of chromosphere is enhanced and plages appear (e.g., Linsky et al. 1979; Foing et al. 1989; Chmielewski 2000; Takeda et al. 2010). Nearly all giant and sub-giant stars ($\log g \leq 4.0$) are not active, unless they belong to close binary systems. This is because they are old and the magnetic braking during their main-sequence lifetime and the star expansion in the red giant phase spin down the star. As a consequence they display a low chromospheric activity (Takeda et al. 2010).

In addition, this clear dividing gap between active and quiescent stars is considered to correspond to Vaughan–Preston gap in Ca II H&K (Vaughan & Preston 1980). Martínez-Arnáiz et al. (2011) reported that the Vaughan–Preston gap is also dividing in two separate classes stars with large emission flux and those with small emission flux in other chromospheric lines like $H\alpha$. It is widely accepted that the differences of stellar age and dynamo regimes are deeply related to existence of this gap between active and quiescent stars (e.g., Durney et al. 1981; Noyes et al. 1984; Böhm-Vitense 2007; Pace et al. 2009; Martínez-Arnáiz et al. 2011). It is also believed that nanoflare heating, which is supposed to be one of the main heating mechanism of the stellar outer atmospheres, contributes to form the gap (Martínez-Arnáiz et al. 2011).

As apparent from Figure 6, KIC6934317 turns out to be a relatively active star, in spite of its low lithium abundance (see Section 4.5). This figure also indicates that 59Vir is an active star, and 61Vir and the Sun are not active stars. These results of 59Vir, 61Vir, and the Sun are consistent with the findings of previous researches (e.g. Anderson et al. 2010, Takeda et al. 2012).

Martínez-Arnáiz et al. (2011) plotted the emission flux in $H\alpha$ versus $B - V$, and displayed the existence of the Vaughan–Preston gap. On the basis of that relation, G-type stars above the gap (active stars) have $\log F_{H\alpha}^{\text{em}} \sim 6 - 7$. With a $\log F_{H\alpha}^{\text{em}} = 6.3$ and $(B - V)_0 \sim 0.64$ (See Section 3.3 and Table 5), KIC6934317 is located above the gap, among the very active stars where strong flares are frequent.

The comparison between our results of emission flux in Table 5 (KIC6934317 has an excess $H\alpha$ flux as compared to Ca II IRT fluxes.) and the results in Martínez-Arnáiz et al. (2011) (A star above the Vaughan–Preston gap has an excess of $H\alpha$ flux with respect to Ca II IRT fluxes.) also shows that this star belongs to the active star group above the gap.

X-ray flux is widely used as a measure of coronal activity and a direct measure of stellar magnetic activity, because it is unlikely to include contribution from other sources such as basal atmosphere (e.g., Schrijver et al. 1992; Pevtsov et al. 2003; Pizzolato et al. 2003). Martínez-Arnáiz et al. (2011) presented the empirical relationship between $H\alpha$ flux and X-ray flux (F_X), and this empirical relationship is given by the following equation,

$$\log F_X = (-2.98 \pm 0.39) + (1.60 \pm 0.07) \log F_{H\alpha}^{\text{em}}. \quad (9)$$

Using this equation, we estimate that F_X of KIC6934317 is $F_X \sim 1 \times 10^7 \text{ erg cm}^{-2}\text{s}^{-1}$, the X-ray luminosity (L_X) of this star is $L_X \sim 4\pi R_s^2 F_X \sim 8 \times 10^{29} \text{ erg s}^{-1}$, and $\log L_X/L_s$ is ~ -3.6 . In calculating these values, we used the values of $R_s \sim 1.0R_\odot$ and $L_s \sim 0.9L_\odot$, as calculated in Section 3.3.

L_X estimated for KIC6934317 is as large as that of KIC7985370 (an active early G-type main sequence star), which is $L_X = (3 - 7) \times 10^{29} \text{ erg s}^{-1}$ (Fröhlich et al. 2012), and much larger than that of the Sun, which varies from about $5 \times 10^{26} \text{ erg s}^{-1}$ to about $2 \times 10^{27} \text{ erg s}^{-1}$ from the minimum to the maximum of the activity cycle (e.g., Schmitt et al. 1995). Hence KIC6934317 is considered to have high coronal activity.

Nevertheless, we do not find the X-ray counterpart of this star in the ROSAT All-Sky Survey (RASS) Faint Source Catalog (Voges et al. 2000). Indeed, the detection limit of the X-ray flux for the RASS survey is $\sim 2 \times 10^{-13} \text{ erg cm}^{-2}\text{s}^{-1}$ (Schmitt et al. 1995), which

corresponds to the X-ray luminosity of $\sim 2 \times 10^{30}$ erg s $^{-1}$ assuming the distance of ~ 300 pc. This explains why KIC6934317 was not detected by the RASS.

On the basis of the discussions and considerations described in this Section and the results of observations that we mentioned in Section 4.3, KIC6934317 shows high chromospheric and coronal activity and it very likely has large plages. In addition, a star with such a high chromospheric activity is also believed to have large starspots (e.g., Schrijver et al. 1992; Busà et al. 2007; Hall 2008). Therefore, given its high activity level, we believe that KIC6934317 has large starspots which can store a large amount of magnetic energy that cause superflares (Shibata et al. 2013).

5.2. Rotational Velocity and Inclination Angle

The value of $v \sin i$ of KIC6934317 estimated by this spectroscopic observation is ~ 1.91 km s $^{-1}$, R_s estimated in Section 3.3 is $\sim 1.0 R_\odot$, and P_s is about 2.54 days. Assuming that the brightness variation of this star is caused by the rotation of the star with starspots, we estimate rotational velocity (v) as ~ 20 km s $^{-1}$ by using following relation:

$$v = \frac{2\pi R_s}{P_s} \quad (10)$$

We think that the difference between the values of v and $v \sin i$ can be explained by the inclination effect. Once v is estimated, we estimate that i (the stellar inclination angle) is ~ 5.5 deg by the following relation (Frasca et al. 2011, Hirano et al. 2012):

$$i = \arcsin \left[\frac{(v \sin i)_{\text{spec}}}{v} \right] \quad (11)$$

This result suggest that KIC6934317 has a small value of i and is a nearly pole-on star.

We can confirm this inclination effect from another point of view. Figure 7 shows the scatter plot of the superflare amplitude as a function of the amplitude of the brightness variation. The data are taken from Notsu et al. (2013). The solid line corresponds to the analytic relation between the stellar brightness variation amplitude and superflare amplitude for $B=1000$ G (Notsu et al. 2013). The amplitude of the brightness variation of the superflare star is considered to be a good indicator of the starspot coverage. In addition, the energy of the superflare can be estimated with the superflare amplitude and duration time. The dashed line corresponds to the same relation in case of nearly pole-on ($i=2.0$ deg) for $B=1000$ G, assuming that the brightness variation of a star become small as the inclination angle of the star become small. These lines are considered to give an upper limit for the flare amplitude in each inclination angle. These results suggest that i of KIC6934317 is small (nearly pole-on)

and that this star has large starspots generating superflares, though the stellar brightness variation amplitude of this star is small ($\sim 0.1\%$).

5.3. *Binarity*

On the basis of the stellar parameters derived in this study, this star proves to be an early G-type main sequence star. Noyes et al. (1984) argued that the rotational period is correlated with the chromospheric activity, which is known to be an indicator of the magnetic activity of the star. Pallavicini et al. (1981) and Pizzolato et al. (2003) showed that rapidly rotating stars have high coronal and magnetic activity than slowly rotating stars. On the basis of these studies, it is not strange that KIC6934317 show high chromospheric and magnetic activity. This is because KIC6934317 has the high rotational velocity ($v \sim 20 \text{ km s}^{-1}$).

Ayres (1997) discussed the dependence of stellar rotational velocity on age for solar-type stars and presented the following relation,

$$\frac{v}{v_{\text{sun}}} = \left[\frac{t}{t_{\text{sun}}} \right]^{-0.6 \pm 0.1}, \quad (12)$$

where v is the rotational velocity of a star, v_{sun} is the rotational velocity of the Sun ($\sim 1.82 \text{ km s}^{-1}$), t is age of a star, and t_{sun} is the solar age ($\sim 4.6 \text{ [Gyr]}$). Using this relation and rotational velocity of this star ($v \sim 20 \text{ km s}^{-1}$), we can estimate that the age of KIC6934317 is $\sim 100 \text{ Myr}$. This value is incompatible with the value estimated in this observation by using the lithium abundance of this star, and the isochrones (See Section 4.3 and 4.5), though there are a lot of unknown problems about the behavior of lithium abundances in early G-type stars as we mention in Section 4.5, and the ranges of values estimated by using these two methods are wide. Thus, one hypothesis that explains the large rotational velocity and high level of activity would be that this star is a binary which has maintained a high rotation rate thanks to the tidal interaction that has coupled spin and orbit (Walter & Bowyer 1981).

First, we checked the slit viewer images of Subaru/HDS for this star taken simultaneously with the spectra, and we cannot find companions for this star as far as we looked this images.

Second, if a star is a binary star and has a companion, RV of the primary star is expected to change between the observations. We estimate the value of the RV change by using the following relation,

$$f(M) = \frac{(M_2 \sin i)^3}{(M_1 + M_2)^2} = \frac{P_o K_1^3}{2\pi G}, \quad (13)$$

where G is the gravitational constant ($= 6.67 \times 10^{-11} \text{ m}^3\text{s}^{-2}\text{kg}^{-1}$), M_1 is the mass of the primary star, M_2 is that of the companion, and $f(M)$ is the mass function. K_1 is the amplitude of radial velocity variation of the primary star, and P_o is the period of orbital motion of the binary system. Thanks to the parameters and $v \sin i$ derived from our obtained spectrum, we can reasonably assume $i = 5.5 \text{ deg}$ and $M_1 \sim 0.97M_\odot$. In addition, if we suppose that this is a close binary system and these stars are expected to be tidally locked with each other, we can assume that P_o is ~ 2.54 days (equal to the rotation period derived from the brightness variation), and that the value of K_1 is larger than the $v \sin i$ ($\sim 1.91 \text{ km s}^{-1}$). Adopting the minimum value of K_1 , we can derive a minimum mass for the unseen secondary component, $M_2 \sim 0.14M_\odot$.

In this observation, we get 6 frames of spectra of KIC6934317, and the exposure time per frame is 1800 seconds (see Section 2.2). Since a frame was obtained ~ 0.5 hours after the previous frame, RV of the star is expected to change between the frames if this star is a binary. Actually, RV of the star calculated from these six frames are, in order from the time, -12.311 ± 0.034 , -12.279 ± 0.027 , -12.190 ± 0.028 , -12.224 ± 0.030 , -12.218 ± 0.029 , $-12.187 \pm 0.026 \text{ km s}^{-1}$ (As we explained in Section 4.2, RV of the star derived from the spectra obtained by integrating all frames of spectra of this star is $-12.238 \pm 0.018 \text{ km s}^{-1}$). The difference between the values of RV of the first frame and the last frame is $0.124 \pm 0.080 \text{ km s}^{-1}$, and thus RV of this star is supposed to change between the first and the last frames. Considering the minimum value of K_1 described in the former paragraph and the time interval between the two frames, however, we cannot claim that this star is definitely a binary. This is because the period of observation is small and because the values of RV change are very small. Especially, the values of RV of last four frames are almost the same values within the ranges of errors. In the future we will observe KIC6934317 again and estimate the change of RV between the observations in detail to investigate whether this star is a binary or not.

6. Summary

In this paper, we present the results of the analysis of a high-resolution spectrum of KIC6934317, a star which displays many strong white-light flares (superflares) in the high-precision Kepler light curve. We measured the core depth and emission flux of Ca II infrared triplet lines and H α line in order to investigate the chromospheric activity and the presence of starspots. Our analysis shows that KIC6934317 has high chromospheric activity, in spite of the low lithium abundance and the small amplitude of the rotational modulation. Using the empirical relations between flux of chromospheric lines and X-ray flux, it should also have a much higher coronal activity than that of the Sun. We believe that the low amplitude of the rotational modulation evident in the Kepler light curve is due only to foreshortening effects

and that this star has actually large starspots which can store a large amount of magnetic energy that can generate superflares. We also estimated some stellar parameters, such as T_{eff} , $\log g$, $[\text{Fe}/\text{H}]$, $v \sin i$, and RV. We confirmed that this star is an early G-type main sequence star, on the basis of these parameters. The value of $v \sin i$ of KIC6934317 is $\sim 1.91 \text{ km s}^{-1}$, though v is estimated to be $\sim 20 \text{ km s}^{-1}$ by using the period of the brightness variation as the rotation period, and R_s of this star. This difference between the values of $v \sin i$ and v can be explained by small inclination angle (nearly pole-on). The amplitude of the brightness variation of superflare stars is considered to correspond to the spot coverage, and it is known to correlate with the superflare amplitude, which corresponds to the energy of superflare. The relation between the superflare amplitude and the brightness variation amplitude in this star is also found to be explained by the effect of small inclination angle. On the basis of the lithium abundance and isochrones, it is implied that the age of this star is more than about a few Gyr, though the problem of the strong activity at such a high age remains unsolved.

This study is based on observational data collected at Subaru Telescope, which is operated by the National Astronomical Observatory of Japan. We are grateful to Dr. Akito Tajitsu and other staffs of the Subaru Telescope for making large contributions in carrying out our observation. We further thank Dr. Kazuhiro Sekiguchi (NAOJ) and Dr. Yoichi Takeda (NAOJ) for useful advices. Kepler was selected as the tenth Discovery mission. Funding for this mission is provided by the NASA Science Mission Directorate. The Kepler data presented in this paper were obtained from the Multimission Archive at STScI. This work was supported by the Grant-in-Aid from the Ministry of Education, Culture, Sports, Science and Technology of Japan (No. 25287039).

References

- Aihara, H. et al. 2011, ApJS, 193, 29
- Alonso, A., Arribas, S., & Martinez-Roger, C. 1996, A&A, 313, 873
- Anderson, R. I., Reiners, A., Solanki, S. K. 2011, A&A, 522, A81
- Asplund, M., Grevesse, N., Sauval, A. J., & Scott, P. 2009, ARA&A, 47, 481
- Ayres, T. R., 1997, J. Geophys. Res., 102, 1641

- Balona, L. A. 2012, MNRAS, 423, 3420
- Basri, G., et al. 2011, AJ, 141, 20
- Biazzo, K., Frasca, A., Catalano, S., & Marilli, E. 2007, Astronomische Nachrichten, 328, 938
- Böhm-Vitense, E. 2007, ApJ, 657, 486
- Brown, T.M., Latham, D. W., Everett, M. E., & Esquerdo, G. A. 2011, ApJ, 142, 112
- Busà, I., Cuadrado, R. A., Terranegra, L., Andretta, V., & Gomez, M. T. 2007, A&A, 466, 1089
- Cardelli, J. A., Clayton, G. C., & Mathis, J. S. 1989, ApJ, 345, 245
- Casagrande, L., Ramírez, I., Meléndez, J., Bessell, M., & Asplund, M. 2010, A&A, 512, A54
- Cauzzi, G., et al. 2008, A&A, 480, 515
- Chmielewski, Y. 2000, A&A, 353, 666
- Debosscher, J., Blomme, J., Aerts, C., & De Ridder, J. 2011, A&A, 529, A89
- Durney, B.R., Mihalas, D., & Robinson, R. D. 1981, PASP, 93, 537
- Everett, M. E., Howell, S. B., & Kinemuchi, K. 2012, PASP, 124, 316
- Foing, B. H., Crivellari, L., Vladilo, G., Rebolo, R., Beckman, J. E., 1989, A&AS, 80, 189
- Frasca, A., & Catalano, S. 1994, A&A, 284, 883
- Frasca, A., Biazzo, K., Kóvári, Z., Marilli, E., & Çakırlı, Ö. 2010, A&A, 518, A48
- Frasca, A., Fröhlich, H.-E., Bonanno, A., Catanzaro, G., Biazzo, K., & Molenda-Żakowicz, J. 2011, A&A, 532A, 81F
- Fröhlich, H.-E., Frasca, A., Catanzaro, G., Bonanno, A., Corsaro, E., Molenda-Żakowicz, J., Klutsch, A., & Montes, D. 2012, A&A, 543, A146
- Girardi, L., Bressan, A., Bertelli, G., & Chiosi, C. 2000, A&AS, 141, 371

- Gray, D. F. 2005, *The Observation and Analysis of Stellar Photospheres*, 3rd ed. (Cambridge: Cambridge University Press)
- Hall, J.C. 1996, *PASP*, 108, 313
- Hall, J. C. 2008, *Living review in Solar Phys*, 5, 2
- Harrison, T. E., Coughlin, J. L., Ule, N. M., & Lopez-Morales, M. 2012, *AJ*, 143, 4
- Herbig, G.H. 1985, *ApJ*, 289, 269
- Hirano, T., Sanchis-Ojeda, R., Takeda, Y., Narita, N., Winn, J. N., Taruya, A., & Suto, Y. 2012, *ApJ*, 756, 66
- Israelian, G., Santos, N. C., Mayor, M., & Rebolo, R. 2004, *A&A*, 414, 601
- Koch, D. G., et al. 2010, *ApJ*, 713, L79
- Kurucz, R. L., Furenlid, I., Brault, J., Testerman, L. 1984, *Solar Flux Atlas from 296 to 1300 nm* (Sunspot, New Mexico: National Solar Observatory) ¹⁰
- Kurucz, R. L. 1993, *Kurucz CD-ROM No.13, Atlas 9 Stellar Atmosphere Programs and 2 Grid* ¹¹
- Kurucz, R. L., & Bell, B. 1995, *Kurucz CD-ROM, No.23* (Harvard-Smithsonian Center for Astrophysics) ¹²
- Linsky, J. L., Hunten, D. M., Sowell, R., Glackin, D. L., & Kelch, W. L. 1979, *ApJS*, 41, 481
- Maehara, H., et al. 2012, *Nature*, 485, 478
- Martínez-Arnáiz, R., López-Santiago, J., Crespo-Chacón, I., & Montes, D. 2011, *MNRAS*, 414, 2629 [Erratum: *MNRAS*, 417, 3100]
- Meylan, T., Furenlid, I., Wiggs, M. S., & Kurucz, R. L. 1993, *ApJS*, 85, 163
- Molenda-Żakowicz, J. et al. 2010, *Astronomische Nachrichten*, 331, 981

¹⁰ Available at <http://kurucz.harvard.edu/SUN.html> .

¹¹ Available at <http://kurucz.harvard.edu/PROGRAMS.html> .

¹² Available at <http://kurucz.harvard.edu/LINELISTS.html> .

- Noguchi, K., et al. 2002, PASJ, 54, 855
- Norris, J. E., Ryan, S. G., & Beers, T. C. 2001, ApJ, 561, 1034
- Notsu, Y., et al. 2013, ApJ, 771, 127
- Noyes, R. W., Hartmann, L. W., Baliunas, S. L., Duncan, D. K., & Vaughan, A. H. 1984, ApJ, 279, 763
- Pace, G., Melendez, J., Pasquini, L., Carraro, G., Danziger, J., François, P., Matteucci, F., & Santos, N.C. 2009, A&A, 499, L9
- Pallavicini, R., Golub, L., Rosner, R., Vaiana, G. S., Ayres, T., & Linsky, J. L. 1981, ApJ, 248, 279
- Pevtsov, A. A., Fisher, G. H., Acton, L. W., Longcope, D. W., Johns-Krull, C. M., Kankelborg, C. C., & Metcalf, T. R. 2003, ApJ, 598, 1387
- Pinsonneault, M. H., An, D., Molenda-Żakowicz, J., & Chaplin, W. J. 2012, ApJS, 199, 30
- Pizzolato, N., Maggio, A., Micela, G., Sciortino, S., & Ventura, P. 2003, A&A, 397, 147
- Priest, E. R. 1981, SOLAR FLARE MAGNETOHYDRODYNAMICS., Gordon and Breach Science Publishers, New York
- Reardon, K. P., Uitenbroek, H., & Cauzzi, G. 2009, A&A, 500, 1239
- Rutten, R.G.M. 1984, A&A, 130, 353
- Ryan, S. G., Kajino, T., Beers, T. C., Suzuki, T. K., Romano, D., Matteucci, F., & Rosolankova, K. 2001, ApJ, 549, 55
- Schmitt, J. H. M. M., Fleming, T. A., & Giampapa, M. S. 1995, ApJ, 450, 392
- Sestito, P. & Randich, S. 2005, A&A, 442, 615
- Soderblom, D. R., Jones, B. F., Balachandran, S., Stauffer, J. R., Duncan, D. K., Fedele, S. B., & Hudon, J. D. 1993a, AJ, 106, 1059
- Soderblom, D. R., Stauffer, J. R., Hudon, J. D., & Jones, B. F. 1993b, ApJS, 85, 315
- Schaefer, B. E., King, J. R., & Deliyannis, C. P. 2000, ApJ, 529, 1026

Schmitt, J. H. M. M., Fleming, T. A., & Giampapa, M. S. 1995, ApJ, 450, 392

Schrijver, C. J., Dobson, A. K., & Radick, R. R. 1992, A&A, 258, 432

Schröder, C., Reiners, A., & Schmitt, J. H. M. M. 2009, A&A, 493, 1099

Shibata, K., et al. 2013, PASJ, 65, 49

Shibata, K., & Magara, T. 2011, Living review in Solar Phys, 8, 6

Shibata, K., & Yokoyama, T. 2002, ApJ, 577, 422

Shibayama, T., et al. 2013, ApJ, submitted

Shine, R.A., & Linsky, J. L. 1972, Sol. Phys., 42, 395

Skrutskie, M. F. 2006, AJ, 131, 1163

Takeda, Y. 1995, PASJ, 47, 287

Takeda, Y. 2007a, PASJ, 59, 335

Takeda, Y., et al. 2005a, PASJ, 57, 13

Takeda, Y., & Kawanomoto, S. 2005, PASJ, 57, 45

Takeda, Y., Kawanomoto, S., Honda, S., Ando, H., & Sakurai, T. 2007b, A&A, 468, 663

Takeda, Y., Honda, S., Kawanomoto, S., Ando, H., & Sakurai, T. 2010, A&A, 515, A93

Takeda, Y., Ohkubo, M., & Sadakane, K. 2002, PASJ, 54, 451

Takeda, Y., Ohkubo, M., Sato, B., Kambe, E., & Sadakane, K. 2005b, PASJ, 57, 27 [Erratum: PASJ, 57, 415]

Takeda, Y., Sato, B., & Murata, D. 2008, PASJ, 60, 781

Takeda, Y., Tajitsu, A., Honda, S., Kawanomoto, S., Ando, H., & Sakurai, T. 2012, PASJ, 64, 130

Valenti, J. A., & Fischer, D. A. 2005, ApJ, 159,141

Vaughan, A. H., & Preston, G. W. 1980, PASP, 92, 385

Voges, W., et al. 2000, IAU Circ., 7432, 1

Walkowicz, L. M., et al. 2011, AJ, 141,50

Walter, F. M., & Bowyer, S. 1981, ApJ, 245, 671

Table 1. Photometric data of KIC6934317

RA*	(J2000)	19 ^h 07 ^m 34 ^s .92
DEC*	(J2000)	+42°29′38″.33
U^\dagger		13.399 ± 0.020 [mag]
B^\dagger		13.191 ± 0.023 [mag]
V^\dagger		12.516 ± 0.017 [mag]
J^\ddagger		10.915 ± 0.019 [mag]
H^\ddagger		10.570 ± 0.017 [mag]
K_s^\ddagger		10.461 ± 0.012 [mag]

Notes

* Brown et al. (2011)

† Everett et al. (2012)

‡ Skrutskie et al. (2006)

Table 2. Atmospheric parameters, projected rotational velocity, radial velocity, and lithium abundance of KIC6934317

Parameter	Value	Reference	
T_{eff}	[K]	5694 ± 25	present work
		5387 ± 200	1
		5710 ± 81	2
		5604 ± 103	3
[Fe/H]		-0.03 ± 0.07	present work
		-0.78 ± 0.5	1
$\log g$		4.42 ± 0.08	present work
		3.8 ± 0.4	1
$v \sin i$	[km s ⁻¹]	1.91	present work
RV	[km s ⁻¹]	-12.238 ± 0.018	present work
A(Li)		1.25	present work

References

(1) Brown et al. (2011)

(2) Pinsonneault et al. (2012) (the SDSS method)

(3) Pinsonneault et al. (2012) (the IRFM method)

Table 3. Atmospheric parameters, projected rotational velocity, radial velocity, and lithium abundance of comparison stars

Name	T_{eff} [K]	[Fe/H]	$\log g$	$v \sin i$ [km s $^{-1}$]	RV [km s $^{-1}$]	W_{Li} [mÅ]	A(Li)	Reference
59Vir	6009 ± 28	0.09 ± 0.06	4.15 ± 0.06	6.27	-26.727 ± 0.026		2.81	present work
	6234		4.60	6.67				1
	6120	0.21	4.25			83.1	2.91	2
	5986		4.25	4.5				3
					-25.9			4
61Vir	5558 ± 15	-0.04 ± 0.06	4.50 ± 0.04	1.38	-7.528 ± 0.027			present work
	5571		4.47	0.46				1
	5720	0.11	4.67			(≤ 2)	(≤ 0.86)	2
	5509		4.51	0.4				3
					-8.1			4

References

(1)Anderson et al. (2010); (2)Takeda & Kawanomoto (2005); (3)Schröder et al. (2009); (4)Takeda et al. (2005a)

Table 4. r_0 of Ca II IRT and H α

Name	$r_0(8498)^*$	$r_0(8542)^*$	$r_0(8662)^*$	$r_0(\text{H}\alpha)^*$
KIC6934317	0.43	0.33	0.37	0.42
59Vir	0.47	0.36	0.37	0.27
61Vir	0.28	0.18	0.19	0.19
Sun	0.30 †	0.19 †	0.19 †	0.18 †

Notes

* r_0 is the residual flux normalized by the continuum at the line core.

† The spectrum of the Sun is obtained by Kurucz et al. (1984). The original resolving power ($R=\lambda/\Delta\lambda$) of this solar spectrum is $\sim 500,000$, but we have brought it to $R\sim 100,000$ to match the resolution of our HDS spectra.

Table 5. The excess equivalent width and the emission flux

Line	W_{λ}^{em} [Å]	F_{λ}^{em} [erg cm ⁻² s ⁻¹]	W_{λ}^{em} [Å]	F_{λ}^{em} [erg cm ⁻² s ⁻¹]	W_{λ}^{em} [Å]	F_{λ}^{em} [erg cm ⁻² s ⁻¹]
	KIC6934317		KIC7985370*		KIC7765135*	
	(The target star)					
Ca II λ 8498	0.09	3.8×10^5	0.26	1.3×10^6	0.26	1.3×10^6
Ca II λ 8542	0.14	6.2×10^5	0.44	2.2×10^6	0.37	1.8×10^6
Ca II λ 8662	0.12	5.5×10^5	0.34	1.7×10^6	0.33	1.6×10^6
H α	0.29	2.0×10^6	0.16 – 0.26	$(1.2 - 2.0) \times 10^6$	0.33	2.5×10^6

Notes

* We use the values of KIC7985370 and KIC7765135 presented in Fröhlich et al. (2012). These stars are early G-type main sequence stars. They are also young, and show high chromospheric activity.

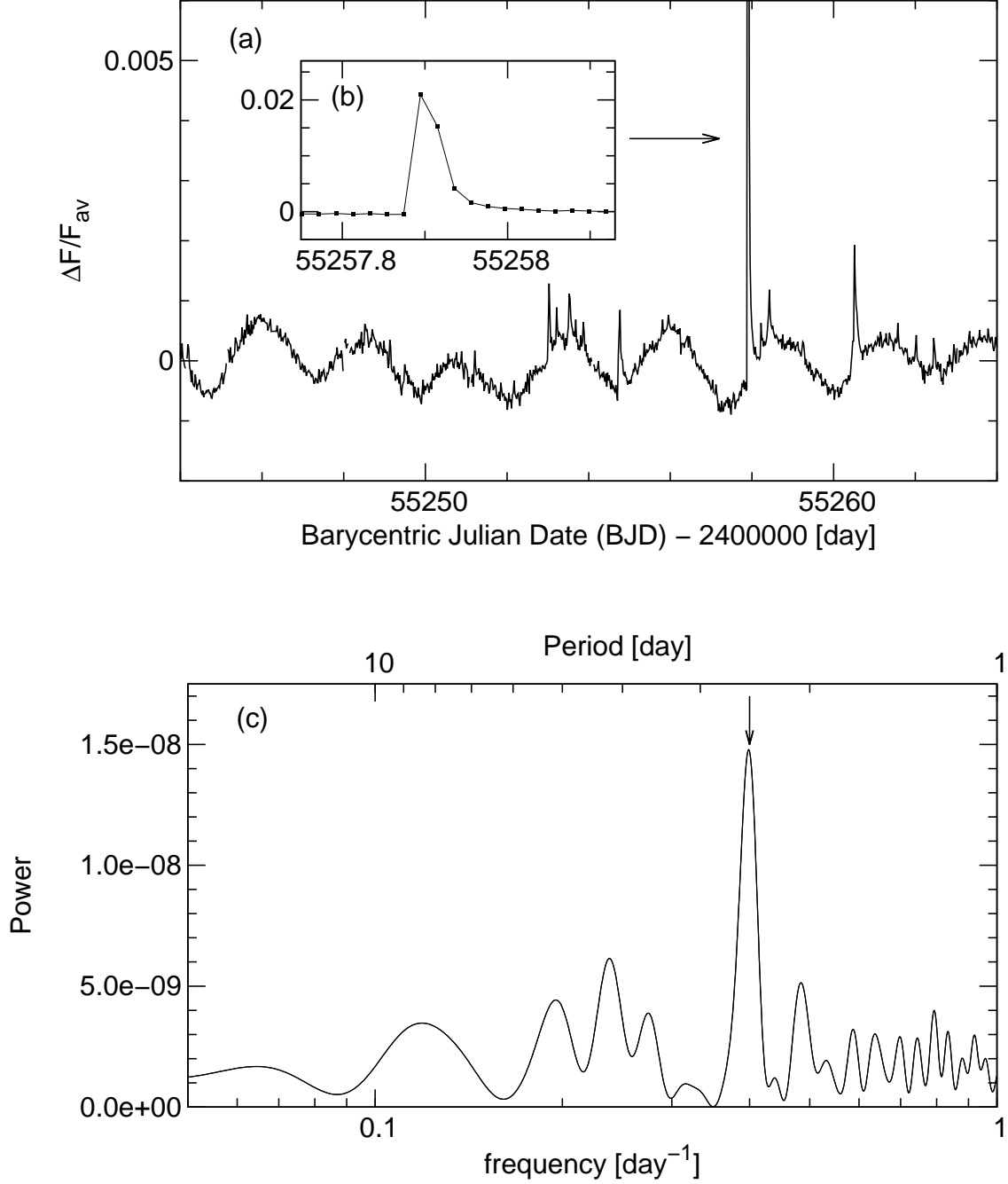


Fig. 1. (a): Lightcurve of KIC6934317 obtained by the Kepler spacecraft. The vertical axis is the brightness variation to the average brightness. We can see quasi-periodic modulation with an about 0.1% amplitude of the total luminosity of the star. (b): The enlarged lightcurve of a superflare observed around BJD 245257.9. The amplitude of this superflare is about 2.1% of the brightness of the star. The duration of the flare is about 0.12 day, and the total radiative energy released during this event is estimated to be about 5.6×10^{34} erg. (c): Power spectra of the light curves of KIC6934317. This figure indicates that the period of the modulation of KIC6934317 (P_s) is 2.54 days.

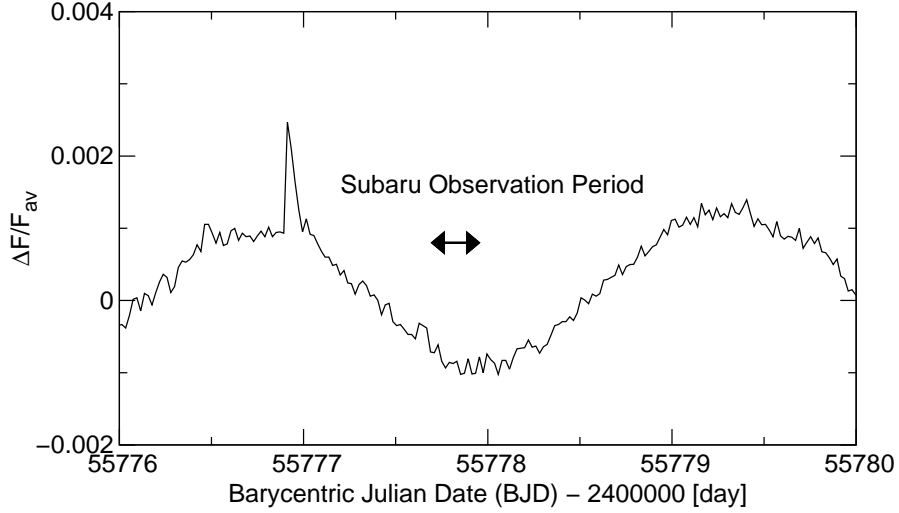


Fig. 2. Lightcurve of KIC6934317 around the period we observed this star with Subaru telescope (August 3, 2012 (HST)). The observation period is in the dark phase of brightness variations. There is a flare about a day before the observation period.

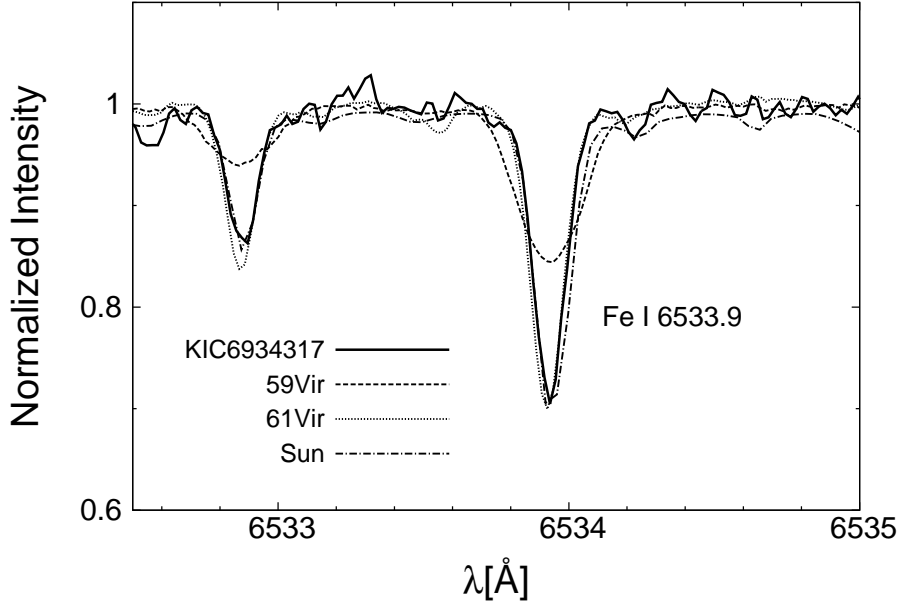


Fig. 3. Normalized spectra of KIC6934317 (solid line), 59Vir (dashed line), 61Vir (dotted line), and the Sun (dash-dotted line) around Fe I 6533.9. The spectrum of the Sun is obtained by Kurucz et al. (1984). The original resolving power ($R = \lambda / \Delta\lambda$) of this solar spectrum is $\sim 500,000$, but we have brought it to $R \sim 100,000$ to match the resolution of our HDS spectra. These spectra show that 59Vir is a fast rotator, while the other stars and the Sun have a low $v \sin i$.

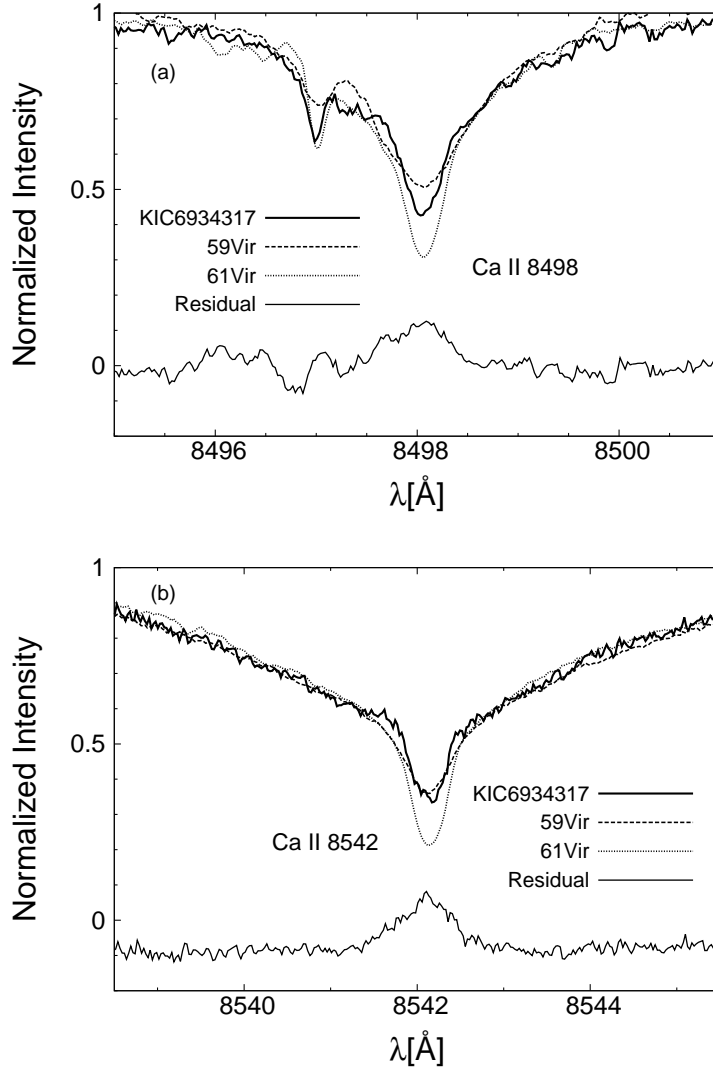


Fig. 4. *Top of each panel:* Normalized spectra of KIC6934317 (thick solid line), 59Vir (dashed line), and 61Vir (dotted line) around the core-regions of Ca II 8498 and 8542. 59Vir and 61Vir are the comparison stars which have strong and weak magnetic fields, respectively (e.g., Anderson et al. 2010). These spectra show that $r_0(8498)$ and $r_0(8542)$ of KIC6934317 are larger than those of 61Vir, and are similar to those of 59Vir. Previous studies (e.g., Linsky et al. 1979; Herbig (1985); Chmielewski 2000) indicate that $r_0(8498)$ and $r_0(8542)$ become large as the star shows high chromospheric activity. Therefore these results suggest that KIC6934317 shows high chromospheric activity like 59Vir. We show the values of $r_0(8498)$ and $r_0(8542)$ of these stars in Table 4. *Bottom of each panel:* The spectrum after subtracting the spectrum of 61Vir (the inactive template star) from KIC6934317 (thin solid line). The residual Ca II 8542 profile is plotted shifted downwards by 0.1 for the sake of clarity. There are clear excess emission around the core-regions of Ca II 8498 and 8542, and we integrated the excess emission regions to get excess equivalent width and emission flux (See Table 5).

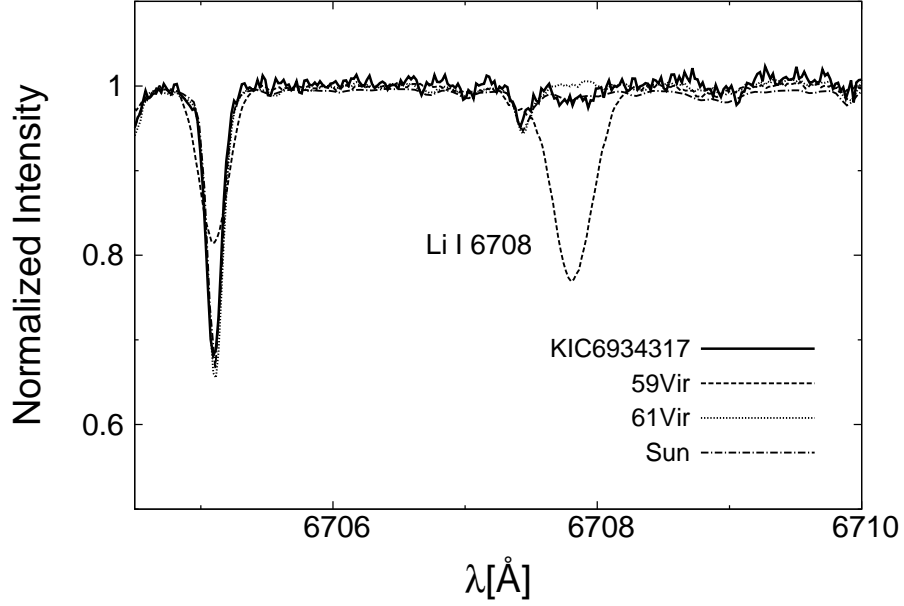


Fig. 5. Normalized spectra of KIC6934317 (solid line), 59Vir (dashed line), 61Vir (dotted line), and the Sun (dash-dotted line) around Li I 6708. The spectrum of the Sun is the same one which we used in Figure 3. According to these spectra, 59Vir has a deep line of Li, and the Li line of 61Vir is absent while that of the Sun and KIC6934317 are very weak and just visible against the noise. In Table 2 and 3, we show the values of lithium abundance ($A(\text{Li})$) of KIC6934317, 59Vir, and 61Vir measured in this study on the basis of the method described in Takeda & Kawanamoto (2005).

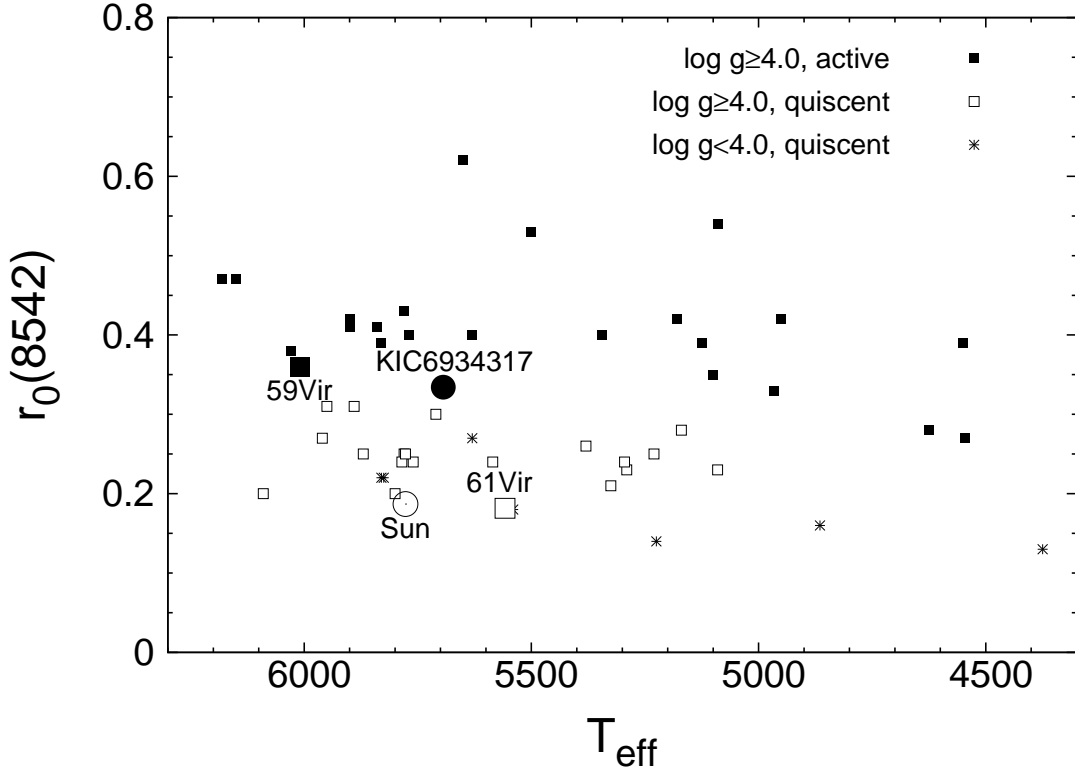


Fig. 6. $r_0(8542)$ (Residual flux normalized by the continuum at the line core of Ca II 8542.) as a function of effective temperature (T_{eff}) of the stars. In this figure, we plot the results of this observation (large symbols), and the data in Chmielewski (2000) (small symbols). Small filled squares represent active dwarf stars ($\log g \geq 4.0$), small open squares indicate quiescent dwarfs ($\log g \geq 4.0$), and small asterisks display evolved (giant or sub-giant) stars which are all considered to be quiescent ($\log g < 4.0$). There appears to be a clear dividing gap between active and quiescent stars which show some slope with effective temperature (e.g., Foing et al. 1989; Chmielewski 2000). The large filled square indicates 59Vir, the large open square represents 61Vir, the large open circle with a point in the center of the circle is the Sun, and the large filled circle is KIC6934317. The position of KIC6934317, 59Vir, 61Vir, and the Sun in this figure indicate that 59Vir is an active star, and 61Vir and the Sun are not active stars, and also suggest that KIC6934317 is a relatively active star.

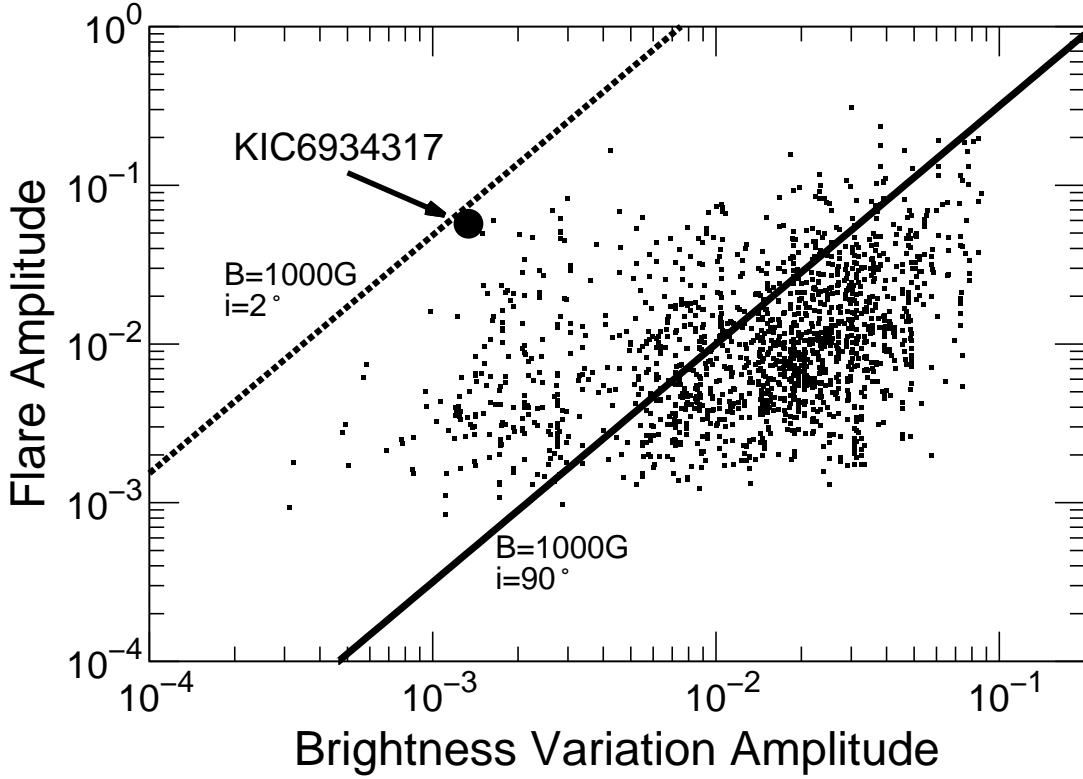


Fig. 7. Scatter plot of superflare amplitude as a function of the amplitude of the brightness variation. The data (small filled squares) are taken from Notsu et al. (2013). The solid line corresponds to the analytic relation between the stellar brightness variation amplitude (corresponding to the starspot coverage) and superflare amplitude (corresponding to the energy of superflare) obtained from Notsu et al. (2013) for $B=1000\text{G}$. The dashed line corresponds to the same relation in the case of nearly pole-on ($i=2.0$ deg) for $B=1000\text{G}$, assuming that the brightness variation of a star become small as the inclination of the star become small. These lines are considered to give an upper limit for the flare amplitude in each inclination. The large filled circle is KIC6934317 (The brightness variation amplitude of KIC6934317 is about 0.1%, and the amplitude of the largest superflare which KIC6934317 exhibits in our data is about 5.7% of the brightness amplitude of the star.). This figure suggests that the inclination angle of KIC6934317 is small (nearly pole-on) and that this star has large starspots.